*Journal of the European Ceramics Society* 7 (1991) 283–293

# Thermo-mechanical Properties and Oxidation Resistance of Zirconia CVI Matrix Composites: 2—Thermal Properties and Oxidation Resistance

J. Minet,* F. Langlais‡ & R. Naslain‡

Laboratoire de Chimie du Solide du CNRS, Université de Bordeaux, 351, Cours de la Libération, 33405 Talence, France

(Received 26 October 1989; revised version received 5 December 1990; accepted 7 December 1990)

**Abstract**

*Zirconia matrix composites, prepared by chemical vapor infiltration (CVI) from preforms (alumina or carbon fibers) having a two- (or pseudo-three-) dimensional character, were studied from a thermal behavior and resistance to oxidation standpoint. The zirconia volume fraction and residual porosity were within the 0·30–0·75 and 0·10–0·25 ranges, respectively. The experiments were carried out up to 1500°C. Thermal expansion is low and almost reversible for the C–$ZrO_2$ composites whereas it is more significant and partly irreversible for the $Al_2O_3$–$ZrO_2$ composites. The $Al_2O_3$–$ZrO_2$ composites exhibit an insulating character above 1000°C, comparable to that of sintered $ZrO_2$, whereas the C–$ZrO_2$ composites have a thermal conductivity equal to that of sintered alumina at $T > 1000$°C. Finally, the resistance to oxidation by air is acceptable at moderate temperatures and for short exposures. In contrast, under more severe conditions, damaging phenomena occur (i.e. grain growth, oxidation of the carbon preform or BN interphase) which are detrimental to the mechanical behavior.*

*Verbundwerkstoffe auf $ZrO_2$-Basis, die aus Vorformen ($Al_2O_3$- oder Kohlenstoffasern) durch CVI hergestellt wurden und eine zwei- bzw. pseudo-dreidimensionale Struktur aufwiesen, wurden auf ihr thermisches Verhalten und ihr Oxidationsverhalten untersucht. Der $ZrO_2$- und der Restporositäts-Volumenanteil lag zwischen 0·30–0·75 bzw. 0·10–0·25. Die Experimente wurden bei Temperaturen bis zu 1500°C durchgeführt. Für die C–$ZrO_2$ Werkstoffe ist die thermische Ausdehnung gering und nahezu reversibel. Die thermische Ausdehnung der $Al_2O_3$–$ZrO_2$ Werkstoffe ist höher und teilweise irreversibel. Über 1000°C zeigen die $Al_2O_3$–$ZrO_2$ Werkstoffe eine Wärmedämmung, die der von gesintertem $ZrO_2$ vergleichbar ist. Die C–$ZrO_2$ Werkstoffe zeigen dagegen die gleiche Wärmeleitfähigkeit wie gesintertes $Al_2O_3$ über 1000°C. Die Oxidationsbeständigkeit in Luft ist bei nicht zu hohen Temperaturen und für kurze Zeiten tolerierbar. Im Gegensatz dazu zeigen sich unter extremeren Bedingungen Schäden (z.B. Kornwachstum, Oxidation der Kohlenstoffvorform oder der BN-Zwischenphase), die sich auf die mechanischen Eigenschaften schädlich auswirken.*

*Des composites à matrice céramique, préparés par CVI à partir de préformes (fibres d'alumine ou de carbone) ayant un caractère bi- (ou pseudo-tri-) dimensionnel, ont été étudiés du point de vue du comportement thermique et de la résistance à l'oxydation. La fraction volumique du zircone et la porosité résiduelle étaient comprises entre 0·30–0·75 et 0·10–0·25, respectivement. Les essais ont été effectués jusqu'à 1500°C. La dilatation thermique est faible et pratiquement réversible pour les composites C–$ZrO_2$ alors qu'elle est plus notable et en partie irréversible pour les composites $Al_2O_3$–$ZrO_2$. La transition $ZrO_2(m) \rightleftharpoons ZrO_2(q)$ semble déplacée légèrement vers les hautes températures. Les composites $Al_2O_3$–$ZrO_2$ présentent au dessus de 1000°C, un caractère isolant comparable à celui de la zircone frittée alors que les composites C–$ZrO_2$ ont une conductivité thermique égale à celle d'une alumine frittée à $T > 1000$°C. Finalement, la résistance à l'oxydation à l'air est acceptable pour des conditions plus sévères, des phénomènes d'endommagement (i.e.*

* Present address: Société Européenne de Propulsion, B.P. 37, 33165 Saint-Médard-en-Jalles, France.
‡ Present address: Laboratoire des Composites Thermostructuraux (UMR 47 CNRS-SEP-UB1), 1–3 Avenue Léonard de Vinci, Europarc, 33600 Pessac, France.



*Journal of the European Ceramic Society* 0955-2219/91/$3.50 

*croissance de grain, oxydation de la préforme de carbone ou de l'interphase BN) se produisent et ont un effet néfaste sur le comportement mécanique.*

## 1 Introduction

Ceramic matrix composites (CMC) based on refractory oxide fibers and matrices (e.g. alumina and zirconia) have not been studied as extensively as their carbide or nitride counterparts. However, their use at high temperatures and under oxygen-rich atmospheres should be obviously more appropriate regarding the outstanding thermal and chemical stability of refractory oxides (alumina and zirconia undergo congruent melting at about 2050°C and 2700°C, respectively). Among the reasons that could explain the rather limited effort of research devoted to $Al_2O_3$ and $ZrO_2$-based CMC are: (i) the higher densities of corundum (3·98 g cm$^{-3}$) and zirconia (5·83 g cm$^{-3}$ for m-$ZrO_2$) with respect to graphite (2·27 cm$^{-3}$) and SiC (3·25 g cm$^{-3}$), whereas most potential applications of CMC are presently in the field of the aerospace industry, (ii) the lack of high-performance fibers suitable for reinforcing oxide matrices at high temperatures and (iii) the well-known brittleness of refractory oxides which implies the use of soft fiber–matrix interphases (acting as crack arresters) in the design of oxide-based CMC (with here the specific requirement that the interphase material has to be stable towards oxidation). On the other hand, the goal of obtaining, through the use of the composite concept, tough materials stable at high temperatures and under oxygen-rich atmospheres, is a very stimulating challenge to researchers. This appears particularly true for $ZrO_2$-based composites, where different toughening mechanisms could be combined (i.e. toughening due to phase transformation, microcracking and fiber pull-out). In that sense, zirconia is probably unique.

As a matter of fact, the number of articles on $ZrO_2$–CMC reinforced with long fibers is very limited, whereas more attention has been paid to the reinforcement of zirconia by whiskers.[1–6] Pujari & Jawed reported the synthesis, according to a powder metallurgy approach, of composites made of tetragonal zirconia polycrystals (TZP) stabilized with 3·5 mol% $Y_2O_3$ and reinforced with 10 wt% of chopped alumina fibers. They mentioned a two-fold increase in fracture toughness over the monolithic TZP.[1] Bender *et al.* have prepared, through a liquid impregnation route (from organometallic precursors) $ZrO_2$–$SiO_2$ and $ZrO_2$–$TiO_2$ matrix composites reinforced with BN-coated SiC fibers (50 vol.%). They established the key role played by the fiber coating in the fracture mechanism (toughening by fiber pull-out) as well as in preventing the matrix–fiber reaction (diffusion barrier). Finally, they reported tensile strengths of 600–700 MPa and toughness of 10–20 MPa m$^{1/2}$ at room temperature.[2] As far as the present authors know, no data have been published on the thermal properties of $ZrO_2$-based fibrous composites.

The aim of the present work was to try to point out the effects of (i) different reinforcements (namely alumina- and carbon-fiber architectures characterized by very different thermal expansion coefficients, thermal diffusivities and oxidation resistances) and (ii) the monoclinic–tetragonal transition of zirconia, on the thermal behavior and oxidation resistance of $ZrO_2$-based CMC. The processing technique and mechanical behavior have been reported in detail elsewhere but were parts of the same programme started a few years ago at University of Bordeaux within the frame of a long-range effort of research on CMC.[7–13]

## 2 Experimental

The samples used in the present study were obtained, starting from different fiber preforms, according to a chemical vapor infiltration (CVI) technique which has been first worked out by Christin *et al.*[11] for SiC-based composites and then extended to various other CMC (namely, $B_4C$, TiC, BN and, more recently, $Al_2O_3$ matrices).[7–13] It has been, in the particular case of zirconia, described in detail elsewhere.[7–9] It will be sufficient to recall here, for the purpose of the discussion, that the precursor of the matrix was a $ZrCl_4$–$H_2$–$CO_2$ mixture and that the densification of the preform was conducted in a CVI laboratory apparatus under the following conditions: $T \approx 910$°C; $p \approx 2$ kPa and $D \approx 100$ cm$^3$ min$^{-1}$.[9] Although the main purpose of this part of the study was not the optimization of toughness, a BN-coating was applied in a few cases to the fiber preforms according to a similar CVI procedure, prior to their densification with zirconia.[14]

Two kinds of reinforcements were selected: (i) alumina-based fibers characterized by an insulating character and a high positive coefficient of thermal expansion (CTE) and (ii) carbon fibers (ex-PAN) characterized by conducting properties and low CTE. Details on the nature of the fiber preforms and derived $ZrO_2$–matrix composites have been given in Part 1 and their main features are shown in Table 1.[10] The open porosity of the preforms ranged, after

**Table 1.** Nature and main characteristics of the fiber preforms and $ZrO_2$–matrix composites

| | *Type 1 specimen* $Al_2O_3(SiO_2/ZrO^2$ | *Type 2 specimen* $(Al_2O_3SiO_2)/ZrO_2$ | *Type 3 specimen* $2D\text{-}(Al_2O_3SiO_2)/ZrO_2$ | *Type 4 specimen* $2D\text{-}C\text{-}C/ZrO_2$ | *Type 5 specimen* $3D\text{-}C\text{-}C/ZrO_2$ |
|---|---|---|---|---|---|
| Fibers | $Al_2O_3$: 97 wt%, $SiO_2$: 3 wt%[a] | $Al_2O_3$: 80 wt%, $SiO_2$: 20 wt%[b] | $Al_2O_3$: 85 wt%, $SiO_2$: 15 wt%[c] | Carbon (ex-PAN)[d] | Carbon (ex-PAN)[d] |
| Fiber binder | Alumina slurry (grain size: 1 $\mu$m) | $Al_2O_3$–$SiO_2$(slurry)[b] | Pyro-BN (CVI) | Pyrocarbon (CVI) | Pyrocarbon (CVI) |
| Texture of the reinforcement | Mat | Short fibers in bulk | 2D Fabrics stacking | 2D Fabrics stacking | 3D Architecture[e] |
| Fiber volume fraction, $V_f$ | 0·17 | 0·10 | 0·37 | 0·30 | 0·20–0·25 |
| Preform porosity $V_{po}$ | 0·60 | 0·85 | 0·53 | 0·50 | 0·70 |
| Zirconia volume fraction, $V_{ZrO_2}$ | 0·44 | 0·75 | 0·31 | 0·38 | 0·62 |
| Residual porosity, $V_p$ | 0·16 | 0·10 | 0·12 | 0·12 | 0·08 |

[a] Saffil fibers (ICI).
[b] Silico–alumina fibers consolidated with silico–alumina binder (Zircar).
[c] Silico–alumina fibers (Sumitomo).
[d] Carbon fibers (Gepem).
[e] Novoltex proprietary preform material (SEP).

consolidation, from 50 to 85% and the residual porosity of the composites after $ZrO_2$ CVI densification, from 8 to 16%. As a result, the volume fraction of zirconia deposited within the pore network was 31–75% depending on the nature of the preforms. Composites referred to as specimens of types 1 to 3 are derived from alumina fiber preforms (type 1: Saffil fiber (ICI) preform/alumina binder; type 2: Zircar fiber preform/alumina–silica binder; type 3: 2D Sumitomo fiber preform consolidated with hex-BN by CVI), whereas specimens of types 4 and 5 are derived from carbon fiber preforms (type 4: 2D carbon fiber preform; type 5: 3D carbon fiber preform developed by SEP) under the trademark Novoltex, both consolidated with pyrocarbon by CVI). Fibers made of pure (or stabilized) zirconia would have been more appropriate than alumina fibers but were not available at that time.[15]

The thermal and oxidation resistance tests were run according to conventional procedures. The thermal expansion experiments (dilatometer type 402 E3, Netzsch), were performed up to 1500°C under an argon atmosphere on samples (50 × 5 × 5 mm) cut in the preforms, parallel to the fiber reinforcement (direction 1), prior to the $ZrO_2$ CVI densification as explained in Part 1.[10]

The thermal diffusivity of a solid can be defined in terms of the transient heat conduction equation:

$$\lambda \partial^2 T/\partial x^2 = C_p \rho \, \partial T/\partial x \qquad (1)$$

where $\lambda$ is the thermal conductivity, $C_p$ the specific heat and $\rho$ the density. The thermal diffusivity $a$ is related to $\lambda$, $C_p$ and $\rho$ by:

$$a = \lambda/C_p\rho \qquad (2)$$

The thermal diffusivity is a more fundamental parameter than the thermal conductivity, from a designer viewpoint, since it is the diffusion constant which is necessary to calculate the spatial propagation of heat in a non-uniform temperature field.[16] The thermal diffusivity measurements were performed with an in-house built apparatus (SEP) on cylindrical samples ($d = 10$ mm; $h = 3$ mm) cut in the preforms either parallel or perpendicular to the fiber reinforcements (directions 1 and 3), prior to the $ZrO_2$ CVI densification, according to a technique which has been described in detail elsewhere.[17] The experiments were run at different temperatures ranging from room temperature to 1500°C under an argon atmosphere, according to the so-called flash method.[18] According to this technique, one face of the specimen is briefly illuminated with a laser flash (duration of the flash less than one microsecond) and the temperature of the rear face is recorded versus time while the heat flux propagates through the solid. If $h$ is the specimen thickness and $t_{1/2}$ the time which is necessary to raise the temperature of the rear face to $T_M/2$ (where $T_M$ is the maximum temperature reached at the rear face due to the heat flux), then the thermal diffusivity is given by:[18]

$$a = 1{\cdot}38(h^2)/(\pi^2 t_{1/2}) \qquad (3)$$

Furthermore, in order to derive the thermal conductivity, $\lambda$, from the thermal diffusivity data, applying eqn (2), the specific heat, $C_p$, and the density, $\rho$, of the solid have to be known. Therefore, density was measured, at room temperature, according to the conventional Archimedes method. Specific

heat was measured by differential scanning calorimetry (DSC) (DSC-30, Mettler) on cylindrical samples ($d = 5$ mm; $h = 1$–3 mm). The two samples, i.e. the composite specimen and an alumina standard, set in two similar crucibles, were heated simultaneously in the same furnace at a constant temperature increase rate $K$ (expressed in K min$^{-1}$), under an atmosphere of nitrogen, from room temperature to a given temperature $T_c$ (with $T_c$ ranging from 70 to 570°C). The heat flux (in mW) at $T_c$, $H^0_{Tc}$, towards the composite specimen, is given by:

$$H^0_{T_c} = -\frac{T_c - T_S}{R_{th}} \quad (4)$$

where $T_c - T_S$ is the difference between the temperature of the composite specimen $T_c$ and that of the standard $T_S$ (both in K) and $R_{th}$ is the thermal resistance between the two specimens (in K/mW). The specific heat $C_p(T_c)$, expressed in J K$^{-1}$ g$^{-1}$, is then calculated according to the following equation:

$$C_p(T_c) = \frac{H^0_{T_c}}{mK} \quad (5)$$

where $m$ is the composite specimen mass.

In order to study the effect of an oxygen-containing gaseous atmosphere on the stability of the composites, tests were run on different samples, i.e. bending test specimens (60 × 12 × 2 mm) or cylindrical specimens ($d = 8$ mm; $h = 8$ mm) cut, as said above, in the preforms prior to $ZrO_2$ CVI densification, either in air or pure oxygen and at a temperature within the range 1100–1200°C. The weight variations of the samples were usually recorded versus time with a microbalance. After cooling, the samples were analyzed by X-ray diffraction (XRD) with Cu-K$\alpha$ radiation, scanning electron microscopy (SEM) as well as Raman spectroscopy microanalysis (RSM)* with a laser beam ($\approx 1\,\mu$m in diameter; Raman MOLE microanalyzer; argon ion laser, 5145 Å emission line).

## 3. Results and Discussion

### 3.1 Thermal expansion

The thermal expansion tests were performed, parallel to the reinforcement layers (direction 1), on three different materials. The first belongs to the composite 1 series but was incompletely densified, i.e. it had a $ZrO_2$ volume fraction of only 0·19 (instead of 0·44 as reported in Table 1) and therefore a rather large residual porosity ($V_p = 0{\cdot}38$). The second is a composite of type 4 and the third a composite of type 5 (with a somewhat lower zirconia volume fraction, i.e. 0·55 instead of 0·62).

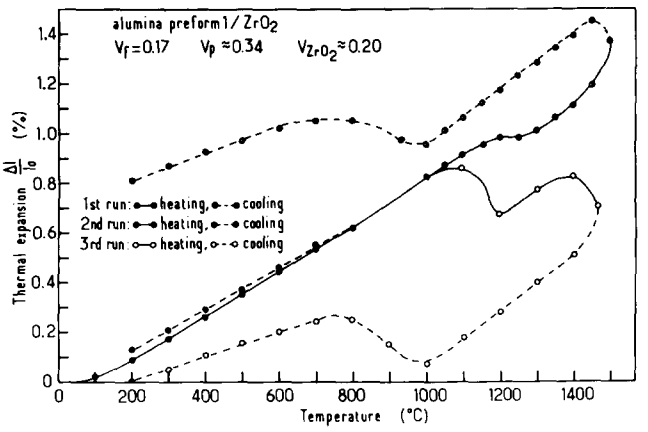


**Fig. 1.** Thermal expansion of an alumina–zirconia composite (type 1) as a function of temperature.

The variations of the thermal expansion $\Delta l/l_0 = (l_T - l_0)/l_0$, where $l_T$ and $l_0$ are the lengths of the specimen at $T$ and ambient temperature respectively, as a function of temperature, are shown in Figs 1–3. Three heating/cooling cycles are given for each material in order to point out the reversible and irreversible evolutions in length of the materials induced by temperature (the irreversible phenomena could be due to microstructural changes occurring: (i) in the fibers when they are heated above their processing temperature, (ii) in the matrix, above the temperature at which it has been infiltrated and/or due as well to (iii) permanent sliding at the fiber matrix interfaces). Assuming that the monoclinic–tetragonal transition of zirconia takes place between 1000 and 1200°C[19] even when zirconia is trapped within a fiber skeleton, the first temperature cycle was limited to 800°C, i.e. well below: (i) the $ZrO_2(m) \rightarrow ZrO_2(t)$ transition, and (ii) the temperatures at which $ZrO_2$ was formed by CVI ($\approx 900$°C), and the preforms processed (900–1100°C for CVI consolidation by pyrocarbon and 1400°C

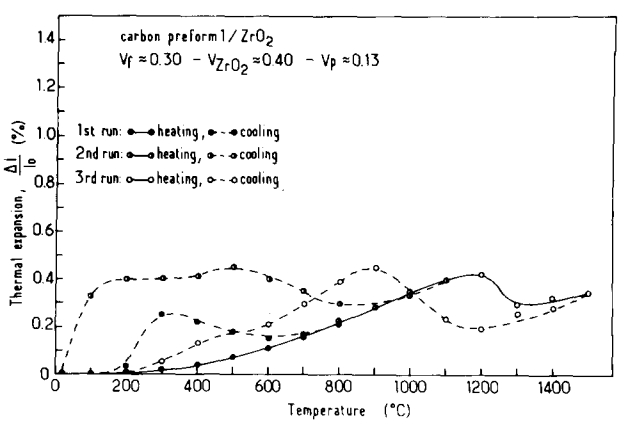


**Fig. 2.** Thermal expansion of a carbon–zirconia composite (type 4) as a function of temperature.

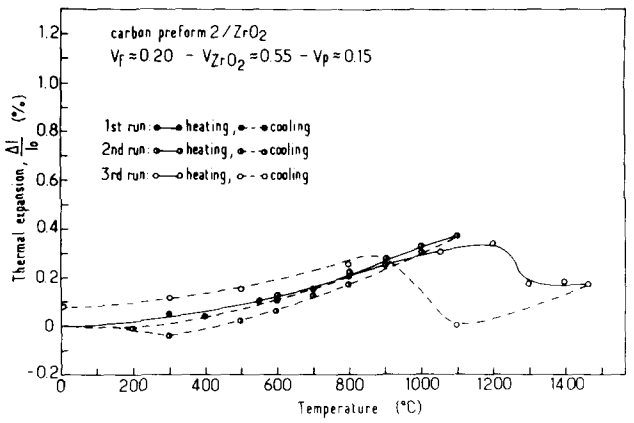


Fig. 3. Thermal expansion of a carbon–zirconia composite (type 5) as a function of temperature.

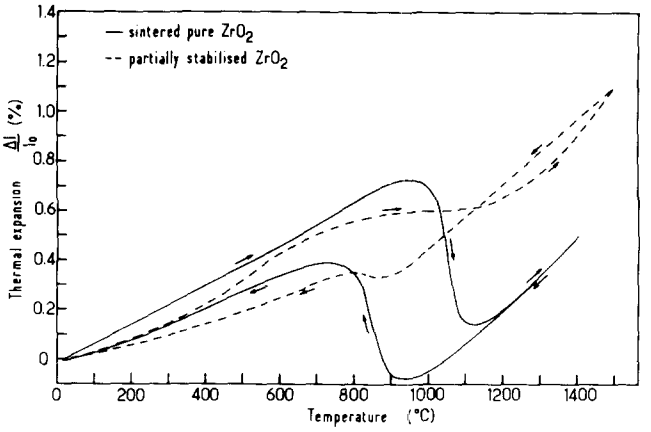


Fig. 4. Thermal expansion of unreinforced zirconia as a function of temperature.

for slurry impregnation and sintering). On the other hand, the second and third temperature cycles usually exhibit an excursion near or above the $ZrO_2(m) \rightarrow ZrO_2(t)$ transition temperature.

Generally speaking, the thermal expansion behavior of the materials is reversible within the 20–800 °C temperature range. Although the $\Delta l_0$–$T$ curves are almost the same on heating and cooling for the composites of types 1 and 5, they appear to be very different at low temperatures for the composite of type 4, which exhibits a significant expansion on cooling between 500 and 200 °C (this expansion disappearing below 200 °C) (Fig. 2).

Extending the temperature cycle up to 1100 °C does not modify significantly these conclusions. However, the hysteresis effect which was almost negligible for the composite of type 5 between ambient temperature and 800 °C is now more pronounced (Fig. 3). In the same manner, the expansion observed on cooling, for the composite of type 4, takes place earlier (i.e. at about 700 °C) and disappears only when approaching ambient temperature (Fig. 2).

The thermal expansion behavior of the composites becomes more or less complex according to the nature of the preform, when the upper limit of the temperature cycle is extended above the $ZrO_2(m) \rightarrow ZrO_2(t)$ transition. The simplest case is that corresponding to the composite of type 5 in which carbon fibers are orientated along three perpendicular directions (Fig. 3). It is characterized by: (i) a hysteresis loop due to the reversible $ZrO_2(m) \rightleftharpoons ZrO_2(t)$ transition which takes place at 1200–1300 °C on heating and at 1100–900 °C on cooling, i.e. in temperature ranges slightly higher than those reported for unreinforced zirconia (Fig. 4),[19,20] and (ii) a small permanent expansion (about +0·1%) when the specimen is cooled back to ambient temperature. A rather similar behavior is apparent from Fig. 2 for the composite of type 4 with a 2D carbon fiber skeleton. However, the expansion effect due to the polymorphic transition of $ZrO_2$ is smaller (a feature which could be simply related to the lower $ZrO_2$ volume fraction). Furthermore, the expansion at low temperatures on cooling, which has been reported for the temperature cycles limited to 800–1100 °C, is found to have almost disappeared after heating at 1500 °C. This feature suggests that further cycling at 1500 °C could result in thermal expansion curves similar to that observed for the composite of type 5 after one single cycle at 1500 °C (Fig. 3). Finally, the material never exhibits a permanent expansion when cooled back to the ambient. Although the reasons that could explain the differences in the thermal behavior of samples 4 and 5, particularly at low temperatures, are still speculative, one parameter which could play an important role is the nature of the fiber preform. In sample 4, it is two-dimensional, whereas it is three-dimensional in sample 5. Furthermore, the carbon fibers themselves may have been processed at different temperatures and may be regarded as more or less stabilized.

As shown in Fig. 1, the thermal expansion curves for the composite deriving from the alumina-based preform (composite of type 1) become much more complex when the temperature cycle is extended up to 1500 °C, with the following main features: (i) during the first heating at high temperatures (cycle 2), the $ZrO_2(m) \rightarrow ZrO_2(t)$ transition is hardly detectable, whereas it is well apparent on cooling as well as on both heating and cooling during the second high-temperature cycle (cycle 3); (ii) the $ZrO_2(m) \rightleftharpoons ZrO_2(t)$ transitions are shifted about 100 °C below those reported for the carbon fiber reinforced composites, i.e. they take place within temperature ranges which are in better agreement with those of unreinforced zirconia (Fig. 4);[20] (iii) finally, after the first heating at 1500 °C, the specimen

**Table 2.** Thermal expansion characteristics of the composites of types 1, 4 and 5 (assuming a $\Delta l/l_0 = f(t)$ linear relation within the temperature range considered)

| *Composites* | *Temperature range (°C)* | *Means* $\alpha_1(K^{-1} \times 10^{-6})$ |
|---|---|---|
| Type 1 (alumina preform) | 200–1000 | 9·2 |
| Type 4 (2D-c–C preform) | 500–1100 | 5·5 |
| Type 5 (3D-C–C preform) | 500–1100 | 3·8 |

has kept a large permanent expansion when cooled back to a temperature close to the ambient (i.e. +0·8% at 200°C).

Although a detailed understanding of the thermal expansion behavior of $ZrO_2$-based fiber composites would obviously require complementary experiments, some general comments can be made on the basis of the present explanatory study. Figures 1–3 show that below the $ZrO_2(m) \rightarrow ZrO_2(t)$ transition the thermal expansion behavior of the composites is neither perfectly reversible nor linear. However, assuming, to a first approximation, a linear $\Delta l/l_0$–$T$ relationship in a given temperature range, CTE can be calculated from the thermal expansion data. The values given in Table 2, shows that the composites with a carbon fiber skeleton have a better dimensional stability than those deriving from the alumina preforms, due to the much lower CTE of the 2D-C–C preform. As already established for other matrices (e.g. glass–ceramics or metals), this effect of the carbon reinforcement on the thermal expansion of $ZrO_2$–matrix composites should be still more pronounced if HM or UHM carbon fibers are used.

On the other hand, the origins of the other phenomena which have been reported here remain a matter of speculation regarding the limited amount of data and samples. Thus, the permanent expansion observed for the composite of type 1, after heating at 1500°C and cooling, could be related to at least two complementary phenomena: (i) the absence of contraction at the $ZrO_2(m) \rightarrow ZrO_2(t)$ on heating which does not balance the expansion on cooling at the reverse transition and (ii) some creep, at high temperatures, of the poorly densified composite (which contains, moreover, a significant amount of silica). However, these two phenomena are no longer observed during the second cycle at 1500°C. Similarly, the expansion on cooling which appears at low temperatures for the composite of type 4 may have to be connected to the strong 2D anisotropy of the material. As a matter of fact, it is not present for the composite of type 5, whose main difference is the occurrence of some fibers bonding the carbon 2D layers together in the third direction.

### 3.2 Thermal diffusivity

The thermal diffusivity measurements were performed on four different materials, parallel (direction 1) or perpendicular (direction 3) to the ceramic fiber layers: composites of type 1 ($V(ZrO_2) = 0{\cdot}40$; $V_p = 0{\cdot}22$), type 2 ($V(ZrO_2) = 0{\cdot}75$; $V_p = 0{\cdot}10$), type 4 ($V(ZrO_2) = 0{\cdot}32$; $V_p = 0{\cdot}15$) and type 5 ($V(ZrO_2) = 0{\cdot}60$; $V_p = 0{\cdot}10$).

The variations of the thermal diffusivities $a_1$ and $a_3$ (measured in a direction parallel or perpendicular to the fiber layers, respectively), as a function of temperature, are shown in Figs 5 and 6.

The thermal diffusivities of the $ZrO_2$–matrix composites decrease regularly as temperature increases. They are lower for the composites derived from the alumina preforms than for those measured on the composites reinforced with a carbon fiber skeleton (carbon fibers consolidated with pyrocarbon), a feature which is a direct result of the insulating and conducting characters of alumina and carbon, respectively. Furthermore, and as shown in Fig. 5, the thermal diffusivity of the $Al_2O_3$ ($SiO_2$)–$ZrO_2$ composites decreases as the volume fraction of zirconia increases, due to the fact that zirconia is a better insulating material. Thus, the

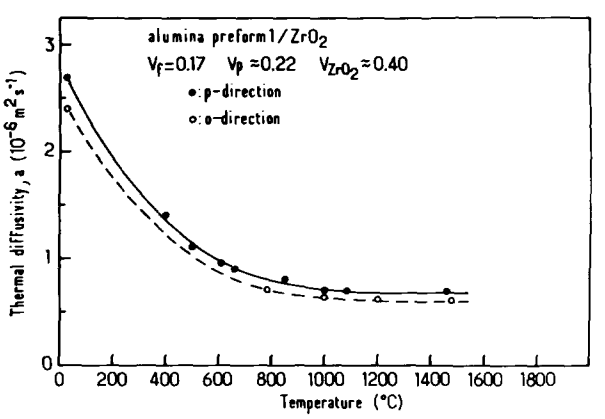


(a)

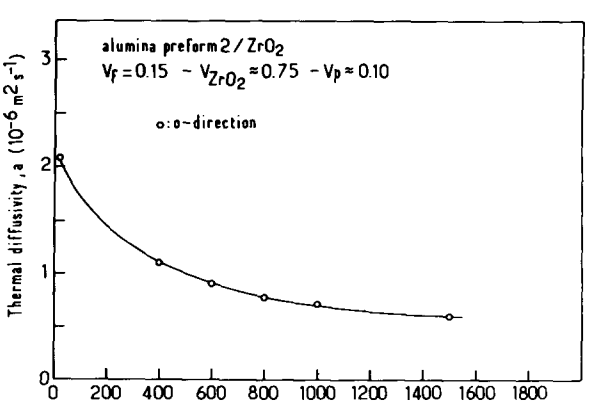


(b)

**Fig. 5.** Thermal diffusivity of alumina–zirconia composites (a) type 1 and (b) type 2 as a function of temperature.

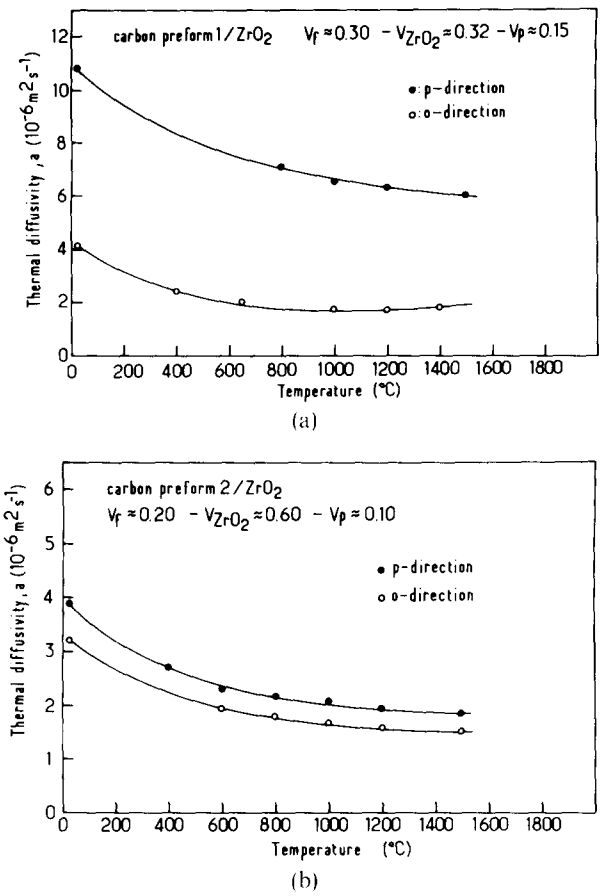


**Fig. 6.** Thermal diffusivity of carbon–zirconia composites (a) type 4 and (b) type 5 as a function of temperature.

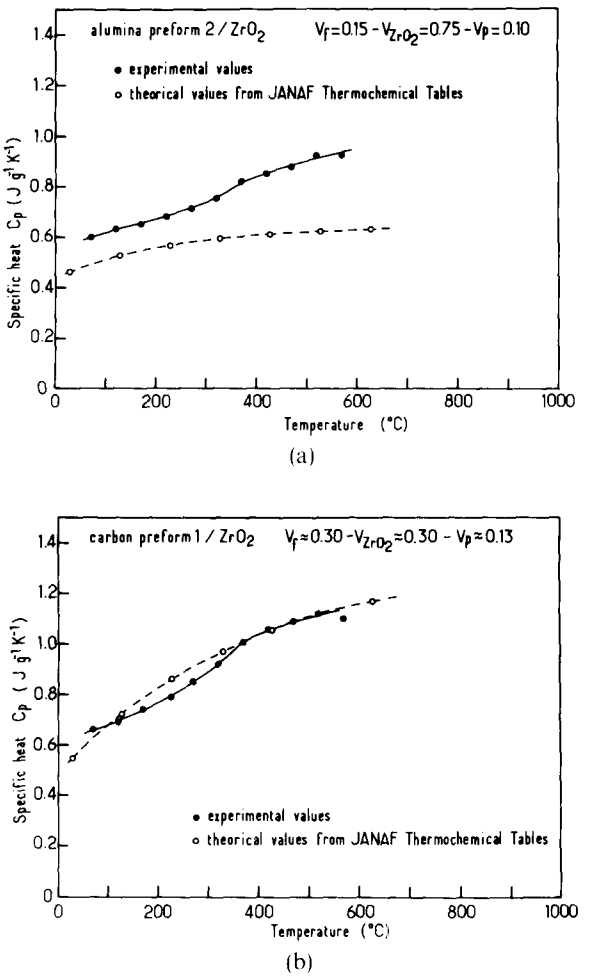


**Fig. 7.** Variations of the specific heat of (a) alumina–zirconia composite (type 2) and (b) carbon–zirconia composite (type 4) as a function of temperature.

composites obtained by $ZrO_2$ densification of $Al_2O_3$ ($SiO_2$) preforms have a lower thermal diffusivity than those derived from the same preforms by $Al_2O_3$ densification. As an example, $a_1 = 4{\cdot}5 \times 10^{-6}$ and $2{\cdot}7 \times 10^{-6}\ m^2\ s^{-1}$ at ambient temperature for composites of type 1, densified according to the same CVI technique by alumina and zirconia, respectively.[13] Finally, the anisotropy of thermal diffusivity of the composites derived from the alumina-based preforms is weak, as could have been predicted from the insulating character of both alumina and zirconia.

In contrast, the thermal diffusivity anisotropy of the composite of type 4, made of a 2D-C–C skeleton densified with zirconia, is much more pronounced, due to the texture of the composite, the conducting character of carbon and the insulating properties of zirconia. The thermal diffusivity is higher in a direction parallel to the carbon fabrics (due to the continuity of the carbon skeleton) than in an orthogonal direction where there is a stacking of alternating layers of conducting and isolating materials. This feature is general for all the composites derived from a 2D-C–C preform. It has been reported already for the 2D-C–C/SiC and 2D-C–C/TiC composites.[21,22] It is even true for the 2D-C–C composites themselves.[23] As could have been predicted, the thermal diffusivity anisotropy of the composite of type 5 is much lower, due to the occurrence of carbon fibers running in a direction perpendicular to the carbon fabrics, a feature which is specific to the Novoltex fiber architecture (Fig. 6). The low values of the thermal diffusivities measured on this composite are due to the high volume fraction (i.e. 0·60) of the isolating $ZrO_2$ matrix.

### 3.3 Specific heat and thermal conductivity

Specific heat measurements have been performed on two different materials, i.e. on composites of types 2 and 4 derived from alumina-based and carbon-based preforms, respectively (Table 1). The variation of the specific heats $C_p$ as a function of temperature is shown in Fig. 7. For both materials, a slight modification of the slope of the curve occurs at about 350°C whose origin is presently unknown.

The specific heat appears to be higher for the composite with a carbon skeleton than for the

composite prepared from the alumina-based preform, whatever the temperature, the gap being higher at high temperatures. This feature is in agreement with the fact that: (i) carbon has itself a higher $C_p$ than both alumina and zirconia and (ii) its $C_p$ increased more rapidly with rising temperatures than those of alumina and zirconia.[25]

Assuming that the specific heat of the composites obeys the rule of mixtures, the $C_p$ values of the composites have been calculated from the compositions of the materials and from the $C_p$ values of the constituents taken from Ref. 25. The calculated $C_p$ values are given in Fig. 7.

It clearly appears from Fig. 7 that there is a rather good agreement between the calculated and measured $C_p$ values for the composite of type 4 (prepared from the 2D-C–C preform). In contrast, for the composite of type 2 (obtained from $Al_2O_3$ ($SiO_2$) preform), the measured $C_p$ values are systematically higher than the calculated values and they increase more rapidly with rising temperatures. These features could result from the fact that (i) both the fibers and their binder are not pure alumina but are made of alumina and silica (silica has not been taken into account in the calculation of $C_p$) and (ii) the $ZrO_2$ matrix deposited by CVI often contains a small amount of free carbon, as established by Minet *et al.*[7,8]

From the measured values of density, thermal diffusivity and specific heat, the thermal conductivity $\lambda$ can be calculated from eqn (2). The variation of $\lambda$ as a function of temperature is shown in Fig. 8 for different $ZrO_2$–matrix composites as well as those for several related monolithic materials (i.e. pyrolytic graphite, sintered alumina and zirconia).

The $Al_2O_3(SiO_2)$–$ZrO_2$ fibrous composites have, at room temperature, thermal conductivities which are very similar in directions parallel and perpendicular to the fiber layers (directions 1 and 3, respectively), as discussed for the thermal diffusivities (i.e. $\lambda_1 = 5$ and $\lambda_3 = 4\,W\,m^{-1}\,K^{-1}$). As the temperature is raised, the thermal conductivities decrease down to values which are close to that of sintered stabilized zirconia at 1500°C. Therefore, the $Al_2O_3(SiO_2)$–$ZrO_2$ fiber composites can be regarded, above about 1000°C, as materials having insulating properties equivalent to those of zirconia. In contrast, and as expected, the composites prepared from carbon fiber preforms have higher thermal conductivities. Moreover, the strong anisotropy which characterizes the thermal diffusivity of the 2D-C–C/$ZrO_2$ composites (type 4) results in a similar anisotropy for the thermal conductivity (since $\rho$ and $C_p$ are volumic properties). As an

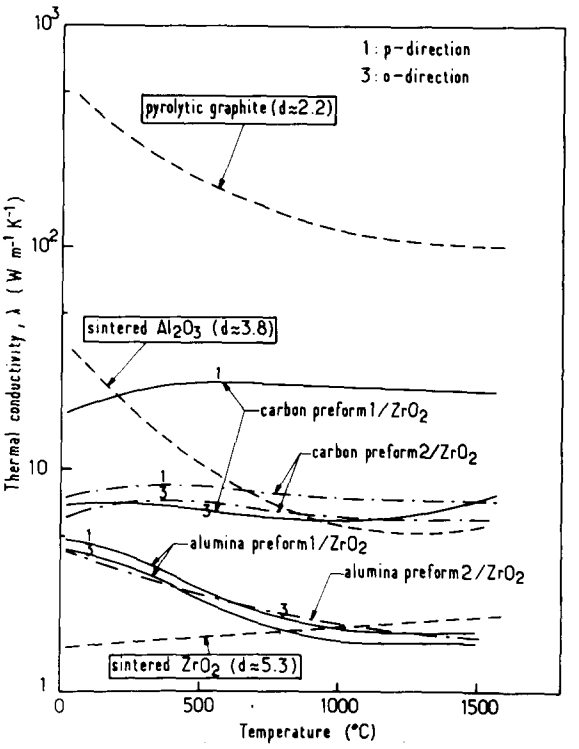


**Fig. 8.** Variations of the thermal conductivity $\lambda$ of zirconia–matrix composite materials versus temperature.

example, at room temperature, $\lambda_1 = 18$ and $\lambda_3 = 7\,W\,m^{-1}\,K^{-1}$. This is no longer the case for the composite of type 5 obtained from the Novoltex preform which exhibits only a weak anisotropy with $\lambda$ values remaining almost constant within the whole 20–1500°C temperature range ($\lambda_1 = 7$–$8$ and $\lambda_3 = 6$–$7\,W\,m^{-1}\,K^{-1}$).

### 3.4 Resistance to oxidation

The oxidation tests were performed on composites prepared either from alumina-based preforms (composite of type 1) or carbon-based preforms (composite of type 4). Moreover, since hex-BN could be a potential interphase material, the tests were extended to composite of type 3.[2,14]

#### *3.4.1 Composites of alumina–zirconia*

Bending test specimens of composite of type 1 ($V(ZrO_2) = 0{\cdot}40$; $V_p = 0{\cdot}20$) were heated at 1300°C in air for 6 h, cooled to ambient temperature and analyzed. Several important phenomena occur during the oxidation test which modify both the composition and microstructure of the $ZrO_2$–matrix (which has been formed at a much lower temperature, i.e. about 900°C). The small amount of free carbon codeposited with zirconia from the $ZrCl_4$–$CO_2$–$H_2$ precursor, as mentioned previously, is burnt off, as illustrated by the evolution of the Raman spectrum (Fig. 9).[8] Simultaneously, the poorly crystallized monoclinic $ZrO_2$–matrix under-

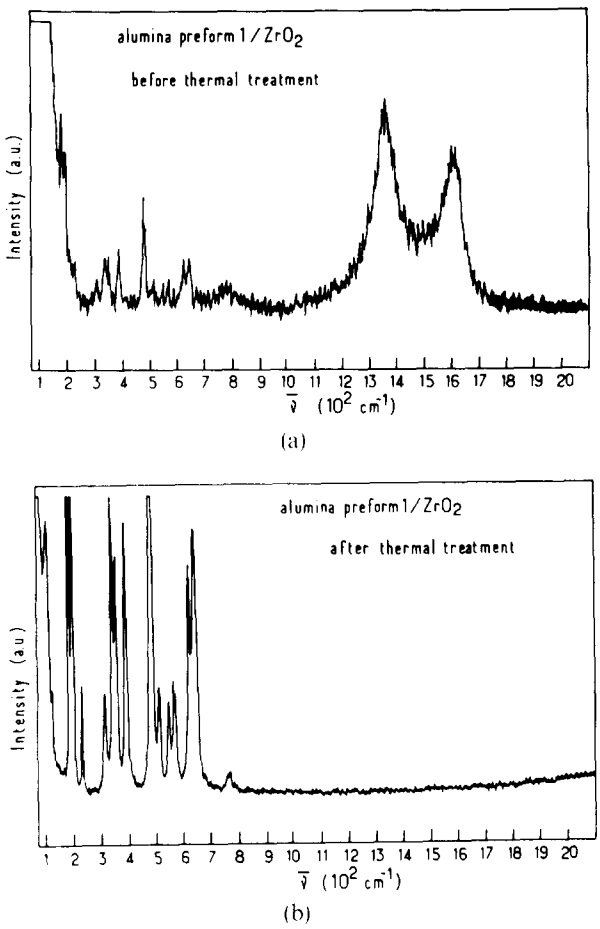


**Fig. 9.** Raman spectra of the zirconia-based matrix in composite of type 1: (a) as prepared and (b) after an oxidation test in air at 1300 C. After the oxidation test, the two broad peaks assigned to carbon have disappeared and the numerous peaks related to zirconia are sharpened.

goes a recrystallization process, as attested by a sharpening of the Raman pattern lines and a coarsening of the microstructure. This evolution of the matrix and simultaneously that of the alumina fibers (not studied here but known to occur under such conditions) results in a significant lowering of the bending strength (of the order of 30–50%).

A coarsening of the microstructures of both the alumina fibers and M-$ZrO_2$ matrix was also observed, after an oxidation test in air at high temperatures (1200°C; 6 h) for the alumina–zirconia composite of type 5. Moreover, and as could have been predicted, an oxidation of the BN-interphase also takes place, as shown in Fig. 10, which gives the variations of the mass of the sample during the test (temperature was first increased up to 1200°C at a rate of 600°C per hour and then it was maintained at this value for 46 h). During the first part of the test (when temperature is raised from ambient to 1200°C), the sample undergoes a small weight loss which could correspond to both outgasing of the material (whose residual porosity is of the order of

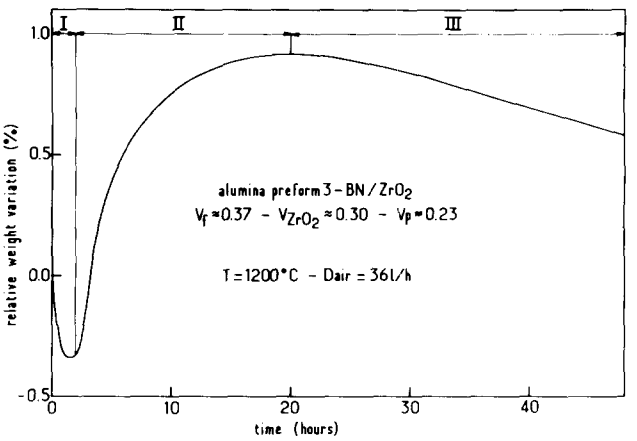


**Fig. 10.** Weight variations of a 2D-$Al_2O_3$(BN)–$ZrO_2$ composite (type 3) during an oxidation test in air at 1200°C.

20%) and an oxidation of the free carbon in the $ZrO_2$-matrix. During the second part of the test, there is a weight increase which is thought to be related to the oxidation of BN, yielding $B_2O_3$. Finally, the sample undergoes a new weight loss (part 3) which could correspond to a slow vaporization of the boron oxide.

It appears from the present study that an aging treatment in air at 1200–1300°C of an alumina–zirconia composite does result in a microstructural change which may be detrimental to some extent to its mechanical behavior (the lack of suitable fibers for high-temperature applications is a well-established feature of the engineering of CMC). Moreover, although BN has been found to be an efficient interphase material for enhancing fiber pull-out and increasing toughness at room temperature in oxide–matrix composites,[2,25] its use in materials which have to sustain long exposures in air at high temperatures, may be questionable unless a protective coating is applied to the whole composite.

### *3.4.2 Composites of carbon–zirconia*

Oxidation tests were also performed on carbon–zirconia composites of type 4 (cylindrical samples: $d = 8$ mm; $h = 8$ mm) in order to assess the effects of temperature, time and oxygen partial pressure on the materials.

A first series of tests was performed in air at 1100°C on samples prepared from a 2D-C–C preform whose open porosity was $V_p \approx 0{\cdot}56$ and which was progressively filled with zirconia up to $V(ZrO_2) = 0{\cdot}30$. As shown in Fig. 11, the oxidation kinetics of the initial 2D-C–C porous preform ($V_{ZrO_2} = 0$) is very rapid, the specimen being totally consumed by oxidation in 90 min. As the volume fraction of zirconia increases, the time necessary to consume the carbon is still very short for

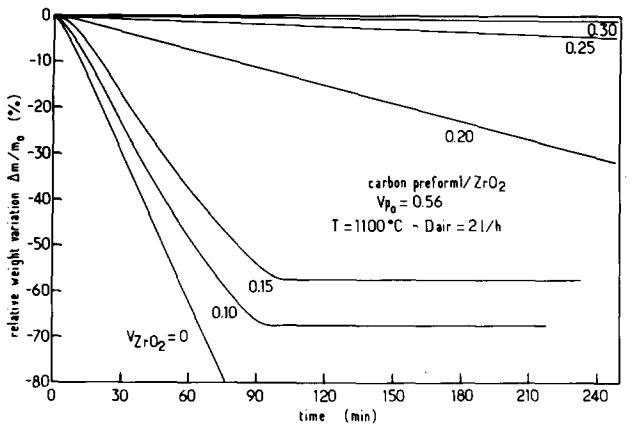


**Fig. 11.** Kinetics of oxidation of a 2D-C–C/$ZrO_2$ composite (type 4) in air at various $V_{ZrO_2}$.

$V(ZrO_2) = 0{\cdot}10$ and $0{\cdot}15$. In contrast, for $V(ZrO_2) > 0{\cdot}20$, a protective effect is observed, the rate of the weight loss decreasing as the volume fraction of $ZrO_2$ increases. For $V(ZrO)_2 = 0{\cdot}30$, the weight loss is less than 2% after 4 h exposure in air at 1100°C, which appears to be a rather remarkable result regarding the poor resistance of carbon to oxidation at such a temperature and the high residual porosity of the composite (i.e. 0·26).

A second series of experiments was run at 1150°C on the same materials (with $V(ZrO_2) = 0{\cdot}30$ and $V_p = 0{\cdot}26$) in order to study the effects of both the gas flow rate and the oxygen partial pressure on the oxidation kinetics (Fig. 12). At a fixed oxygen partial pressure, e.g. for tests performed in air, the weight loss due to oxidation increases linearly versus time, the slope of the $\Delta m/m_0 = f(t)$ straight line (where $\Delta m$ is the weight loss at time $t$ for a sample of initial mass $m_0$) increasing as the gas flow rate is raised. However, in pure oxygen, an initial non-linear regime is observed. Furthermore, at a constant gas flow rate (e.g. 61 liter $h^{-1}$), the weight loss is proportional to the pressure of oxygen (i.e. it is divided by five when pure oxygen is replaced by air).

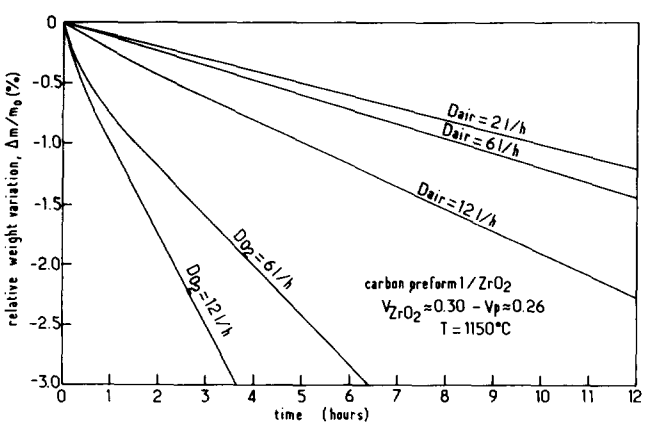


**Fig. 12.** Kinetics of oxidation of 2D-C–C/$ZrO_2$ composites (type 4) as a function of the gas flow rate and partial pressure of oxygen.

Thus, these results show that when carbon fibers are embedded within a zirconia matrix, protection of the fibers by the matrix against oxidation is effective for short exposures at moderate temperatures. In contrast, under more severe oxidation conditions (higher temperatures and/or longer exposures), different damaging mechanisms (i.e. oxidation of the carbon preform and of the interphase, preform–matrix chemical reaction as well as grain growth) take place with a detrimental effect on the mechanical behavior. Some of them could be inhibited through the use of a coating.

## 4 Conclusion

The thermal and oxidation tests which have been performed up to 1500°C on various composites consisting of ceramic fibers (silico–alumina or carbon) embedded by CVI in a zirconia matrix, led to the following main conclusions:

(i) Up to 1000–1100°C, the thermal expansion is reversible whatever the nature of the composite. After a first heating/cooling cycle between 25 and 1500°C, silico–alumina/$ZrO_2$ composites exhibit a residual expansion of the order of 0·8% which might be related to the occurrence of a change in the fibres and/or a chemical reaction between fibers and matrix. However, when reheated up to 1500°C and cooled, silico–alumina/$ZrO_2$ composites behave as zirconia. On the other hand, the thermal expansion of carbon/zirconia is much lower, owing to the very small (if not negative) CTE of carbon fibers, and reversible.

(ii) The thermal conductivity of the carbon/$ZrO_2$ composites at $800 < T < 1500$°C is similar to that of sintered alumina except for the 2D-C–C/$ZrO_2$ material, where it is significantly higher in directions 1 and 2 (the directions parallel to the carbon fiber fabrics) owing to the high thermal conductivity of the carbon fibers themselves. On the other hand, the thermal conductivity of the silico–alumina/$ZrO_2$ composites is similar to that of sintered zirconia within the same temperature range.

(iii) The resistance to oxidation by air is acceptable at moderate temperatures and for short exposures. In contrast under more severe conditions, various damaging phenomena occur, including grain growth of the

silico–alumina fibers and $ZrO_2$–matrix, oxidation of the carbon preform or BN-interphase, which are detrimental to the mechanical properties.

## Acknowledgements

The preforms which have been used in the present study were supplied by SEP and parts of the test were performed in its laboratories. The authors acknowledge the contribution of L. Rabardel and J. Villot for the oxidation tests, and that of M. Couzi and F. Cruege for the Raman microprobe analyses.

## References

1. Pujari, V. K. & Jawed, I., The alumina fibre/tetragonal zirconia polycrystal composite system. *Composites*, **17**(2) (1986) 137–40.
2. Bender, B., Shadwell, D., Bulik, C., Incorvati, L. & Lewis, D., Effect of fiber coatings and composite processing on properties of zirconia-based matrix SiC fiber composites. *Ceram. Bull.*, **65**(2) (1986) 363–9.
3. Claussen, N. & Petzow, G., Whisker-reinforced zirconia-toughened ceramics. In *Tailoring Multiphase and Composite Ceramics, Mater. Sci. Res.*, Vol. 20, ed. R. E. Tressler *et al.*, 1986, pp. 649–62.
4. Claussen, N. & Petzow, G., Whisker-reinforced oxide ceramics. *J. de Physique, Colloque* $C_1$, *Suppl. No. 2*, **47** (1986) $C_1$-693–$C_1$-702.
5. Grewe, H., Dreyer, K. & Kolaska, J., Whisker-reinforced ceramics. *Cfi/Ber.* **8/9** (1987) 303–17.
6. Mazerolles, L., Michel, D. & Portier, R., Microstructure and mechanical behaviour of $Al_2O_3$–$ZrO_2(Y_2O_3)$ oriented eutectics. *J. de Physique, Colloque* $C_1$, *Suppl. No. 2*, **47** (1986) $C_1$-335–$C_1$-339.
7. Minet, J., Langlais, F., Naslain, R. & Bernard, C., On the CVD of zirconia from $ZrCl_4$–$H_2$–$CO_2$–Ar gas mixture: 1—Thermodynamic approach. *J. Less-Common Met.*, **119** (1986) 219–35.
8. Minet, J., Langlais, F. & Naslain, R., On the CVD of zirconia from $ZrCl_4$–$H_2$–$CO_2$–Ar gas mixture: 2—An experimental approach. *J. Less-Common Met.*, **132** (1987) 273–87.
9. Minet, J., Langlais, F. & Naslain, R., Chemical vapor infiltration of zirconia within the pore network of fibrous ceramic materials from $ZrCl_4$–$H_2$–$CO_2$. *Gas Mixtures, Composite Science and Technology*, **37**(1–3) (1990) 79–107.
10. Minet, J., Langlais, F., Quenisset, J. M. & Naslain, R., Thermo-mechanical properties and resistance to oxidation of zirconia CVI matrix composites: 1—Mechanical behavior. *J. Eur. Ceram. Soc.*, **5** (1989) 341–56.
11. Christin, F., Naslain, R. & Bernard, C., A thermodynamic and experimental approach of silicon carbide CVD. Application to the CVD-infiltration of porous composites. In *Proc. Int. Conf. CVD*, ed. T. O. Sedwick & H. Lydbin. The Electrochemical Society, Princeton, 1979, pp. 499–514.
12. Naslain, R. & Langlais, F., CVD-Processing of ceramic composite materials. In *Tailoring Multiphase and Composite Ceramics, Mater. Sci. Res.*, Vol. 20, ed. R. E. Tressler *et al.*, 1986, pp. 145–64.
13. Colmet, R., Lhermitte-Sebire, I. & Naslain, R., Fibrous alumina–alumina composite materials obtained according to a CVI-technique. *Adv. Ceram. Mater.*, **1**(2) (1986) 185–91.
14. Hannache, H., Naslain, R. & Bernard, C., Boron nitride chemical vapour infiltration of fibrous materials from $BCl_3$ $NH_3$ $H_2$ or $BF_3$–$NH_3$–$H_2$ mixtures: A thermodynamic and experimental approach. *J. Less-Common Met.*, **95** (1983) 221–46.
15. Marshall, D. B., Lange, F. F. & Morgan, P. D., High strength zirconia fibers. *J. Am. Ceram. Soc.*, **70**(9) (1987) C187–C188.
16. Hasselmann, D. P. H., Tailoring of the thermal transport properties and thermal shock resistance of structural ceramics. In *Tailoring Multiphase and Composite Ceramics, Mater. Sci. Res.*, Vol. 20, ed. R. E. Tressler *et al.*, 1986, pp. 731–54.
17. Taylor, R., *J. Phys. Experiments, Sciences Instruments*, **13** (1980) 1–7.
18. Parker, W. J., Jenkins, R. J., Butler, C. P. & Abbot, G. L., Flash method of determining thermal diffusivity, heat capacity and thermal conductivity. *J. Appl. Phys.*, **32**(9) (1961) 1679–84.
19. Stevens, R., Zirconia and zirconia ceramics. Magnesium Elektron Ltd, Twickenham, July 1986.
20. Heuer, A. H., *Science and Technology of Zirconia*, The American Ceramic Society, 1981.
21. Christin, F., The C–C/Si composites: A new family of materials for high temperature applications. Thesis 641, University of Bordeaux, 1979, pp. 99–102.
22. Rossignol, J. Y., On the ceramic–ceramic composites made of a 2D-carbon fiber reinforcement densified by CVI by hybrid carbon–carbide or carbon nitride matrices. Thesis 833, University of Bordeaux, 1985, pp. 39–41.
23. Broquere, B., Buttazzoni, B. & Choury, J. J., The carbon carbon composites and their industrial applications. In *Introduction to Composite Materials*, ed. R. Naslain, CNRS-Editions/IMC, Bordeaux, 1985, Chapter 17, pp. 405–38.
24. Stull, D. R. & Prophet, H., *Janaf Thermochemical Tables*, 2nd Edn. NSRDS-NBS 37, 1971.
25. Rice, R. W., BN coating of ceramic fibers for ceramic fiber composites. US Patent 4, 642, 271, 10 February 1987.